https://doi.org/10.5194/egusphere-2023-3118
Preprint. Discussion started: 8 January 2024

A double-Manning approach to compute robust rating curves and hydraulic geometries

Andrew D. Wickert[1,2,3], Jabari C. Jones[1,2,4], and Gene-Hua Crystal Ng[1,2]

[1]Saint Anthony Falls Laboratory, University of Minnesota, Minneapolis, MN 55414, USA
[2]Department of Earth and Environmental Sciences, University of Minnesota, Minneapolis, MN 55455, USA
[3]Sektion 4.6: Geomorphologie, Deutsches GeoForschungsZentrum (GFZ), Potsdam, 14473, Germany
[4]Department of Earth and Oceanographic Science, Bowdoin College, Brunswick, ME 04011, USA

Correspondence: Andrew Wickert (awickert@umn.edu)

Abstract.

Rating curves describe river discharge as a function of water-surface elevation ("stage"), and are applied globally for stream monitoring, flood-hazard prediction, and water-resources assessment. Because most rating curves are empirical, they typically require years of data collection and are easily affected by changes in channel hydraulic geometry. Here we present a straightforward strategy based on Manning's equation to address both of these issues. This "double-Manning" approach employs Manning's equation for flow in and above the channel and a Manning-inspired power-law relationship for flows across the floodplain. When applied to data from established stream gauges, we can solve for Manning's n, channel-bank height, and two floodplain-flow parameters. When applied to limited data from a field campaign, constraints from Manning's equation and the surveyed cross section permit a robust fit that matches ground truth. Using these double-Manning fits, we can dynamically adjust the rating curve to account for channel width, depth, and/or slope evolution. Such rating-curve flexibility, combined with a formulation based in flow mechanics, enables predictions amidst coupled hydrologic–geomorphic change, which increasingly occurs as climate warms and humans modify the land surface and subsurface. Open-source software with example implementations is available via GitHub, Zenodo, and PyPI.

1 Introduction

Hydrologists routinely measure river stage – water-surface elevation above an arbitrary datum – and convert it into discharge – the volume of water passing through a cross section per unit time (World Meteorological Organization, 2010b). Both variables are useful. Stage informs flood hazard and can be used together with streambed elevation to compute water-induced shear stresses that produce turbulence, transport sediment, and shape the stream – including its aquatic habitat (Van Steeter and Pitlick, 1998; Pitlick and Van Steeter, 1998; Luppi et al., 2009; Buahin et al., 2017). Discharge informs water supply and can be linked with catchment-scale hydrological water balances and processes (e.g., Somers et al., 2018; Hut et al., 2022).

Measuring stage requires a straightforward distance measurement. Automated technologies often measure stage; such devices include bubblers, floats, radar systems (Baffaut et al., 2020), pressure transducers (World Meteorological Organization, 2010a; Sauer and Turnipseed, 2010; Quezada et al., 2023), laser rangefinders (Paul et al., 2020), ultrasonic rangefinders (Kruger

https://doi.org/10.5194/egusphere-2023-3118
Preprint. Discussion started: 8 January 2024

et al., 2016), and cameras facing incremented staff gauges (Noto et al., 2022). Where automated methods are not used, measuring stage requires only a visual reading of a staff gauge. Measuring discharge, on the other hand, typically requires either a tracer-dilution test or combined cross-sectional geometry and flow-velocity distribution. Though alternative modeling (Kean and Smith, 2005, 2010) and monitoring (Harpold et al., 2006; Tauro et al., 2016) approaches have been proposed and demonstrated, practicing hydrologists continue to make the overwhelming majority of these measurements by hand (Turnipseed and Sauer, 2010; World Meteorological Organization, 2010a).

As a natural result of the measurement logistics, we posses dense records of stage but sparse records of discharge. Fortunately, higher water is deeper and flows faster. Therefore, assuming no changes in river-channel (and, if present, floodplain) hydraulic geometry, discharge increases monotonically with stage.

By applying this knowledge, hydrologists have developed so-called "rating curves" – mathematical expressions for discharge as a function of stage – for rivers around the world. Most such stage–discharge relationships are fit with a power-law function with a stage offset (e.g., Leopold and Maddock, 1953; Petersen-Øverleir, 2005; Schmidt and Yen, 2008; World Meteorological Organization, 2010b; Hamilton et al., 2016; Hrafnkelsson et al., 2022):

$$Q = k\,(z_s - z_b)^P\,. \tag{1}$$

Here, Q is water discharge, k is a coefficient, z_s is stage, z_b is the stage at which $Q = 0$ (measuered from the same datum as z_s; our subscript b indicates the channel bed), and P is an emprically derived exponent. This power-law form generalizes Manning's equation to include the ability to adjust (via its coefficient and exponent) to a range of hydraulic geometries (e.g., Petersen-Øverleir, 2005; Schmidt and Yen, 2008; World Meteorological Organization, 2010b).

Scientists have expanded from this simple starting point in two major directions: hydrodynamic modeling and enhanced parameterization and/or parameter estimation. Regarding the modeling approaches, Kean and Smith (2005, 2010) developed finite-element methods with field-characterized roughness elements to generate a theoretical approach towards building rating curves without substantial calibration data. Abril and Knight (2004) generated a depth-averaged hydrodynamic model with similar motivation. Numerous studies apply the HEC-RAS (Brunner, 1995) hydraulic modeling package to simulate rating curves based on field-survey data (e.g., Siqueira et al., 2016; Wara et al., 2019; Ghadai et al., 2020; Quintero et al., 2021). Some of these approaches can account for flows that are unsteady and/or nonuniform (along the flow-line direction). Towards the enhanced parameterizations, Mansanarez et al. (2019b) applied a Bayesian approach towards a traditional rating-curve estimation problem to fit rating curves using just a few data points. Hrafnkelsson et al. (2022) permitted the power-law exponent to be its own function of stage and likewise calibrated it in a Bayesian framework.

While effective, these approaches have drawbacks. Quintero et al. (2021) notes the time and work required to prepare the multiple cross sections and their parameters needed for HEC-RAS. Despite the promise of the Kean and Smith (2005, 2010) methods, the complexity of the calculation, the data required, and the lack of a straightforward existing software package have inhibited its uptake. And although Bayesian methods may help to better understand sparse data sets (Mansanarez et al., 2019b), they do not provide fundamental new information. Adding unconstrained parameters can produce better fits – especially when

https://doi.org/10.5194/egusphere-2023-3118
Preprint. Discussion started: 8 January 2024

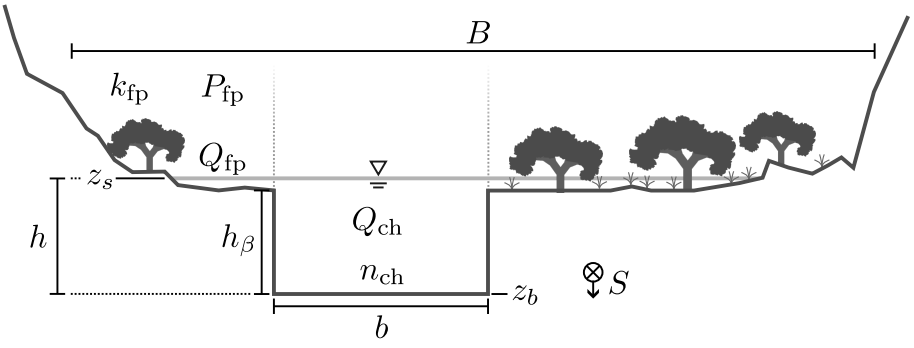

Figure 1. Schematic of the double-Manning approach to relating river stage and discharge. A rectangular channel carries the flow until it goes overbank, at which point it enters the floodplain, whose topography and roughness structure may be more arbitrarily complex. Channel discharge, Q_{ch}, encompasses flow within and (if the water level is high enough) above the channel, as suggested by the fading dotted lines. Floodplain discharge, Q_{fp}, comprises flow to both the left and right of the channel. Other variables: B: valley-bottom width. P_{fp}: floodplain-flow exponent. k_{fp}: floodplain-flow coefficient. z_s: river stage. h: water depth above the channel bed. h_β channel-bank height. n_{ch} Manning's n for flow resistance within the channel. z_b: channel-bed stage – that is, the flow stage at which discharge is 0. S: channel slope. b: channel width. Full discharge $Q = Q_{\mathrm{ch}} + Q_{\mathrm{fp}}$.

the position of such parameters has a basis in the physical system (Hrafnkelsson et al., 2022) – but these are helpful only when sufficient data exist to constrain such a fit.

Here we propose to expand the basic power-law stage–discharge relationship (Equation 1) into a form that:

1. explicitly incorporates both a channel and its floodplain – including the possibility for a break in the rating curve as flows overtop the channel banks (Leopold et al., 1964; Ahilan et al., 2013),
2. enables direct incorporation of often-easily obtained field data to constrain and/or validate the solution,
3. can flexibly incorporate changes in hydraulic geometry and/or roughness as the river cross section evolves, and
4. permits rapid forward and inverse solutions via a prepared software package.

These goals lead us to our so-called "double-Manning" formulation, in which we combine Manning's equation for in-channel flows with a Manning-inspired rating-curve-like power law for overbank flows. This requires steady, uniform flow and, in its present form, a channel whose cross section can be approximated to be rectangular. By adding basic flow mechanics (Gioia and Bombardelli, 2001; Bonetti et al., 2017); constraining solutions against a broader array of field data; and making the solution straightforward and accessible, we see the double-Manning approach as an easily operationalizable "middle road" between the simplified power-law approach (Equation 1) and more complex hydrodynamic models or parameter inversions.

https://doi.org/10.5194/egusphere-2023-3118
Preprint. Discussion started: 8 January 2024

2 Double-Manning Formulation

Here we propose a "double-Manning" approach that applies rating-curve data to calculate flow through the channel and, if water levels are high enough, above the channel and across the floodplain (numerical implementation: Wickert, 2023). In contrast to the traditional single-power-law approach (Equation 1), we subdivide the discharge among the channel and the floodplain (Figure 1). Channel flow comprises both the water that flows through the channel and any water that flows above it. Floodplain flow comprises the flow that crosses the floodplain.

2.1 Channel

For the channel and the region directly above it (Figure 1), we use the classic Manning (1891) formula to solve for velocity as a function of flow depth,

$$\bar{u} = \frac{1}{n_{\mathrm{ch}}} R_h^{2/3} S^{1/2}. \tag{2}$$

Here, n_{ch} is Manning's roughness coefficient within the channel, and R_h is the hydraulic radius, defined as the ratio of the cross-sectional area to the wetted perimeter. Although channels may have complex geometries, a rectangular channel approximation appears reasonable across a range of fluvial geomorphic studies (e.g., Parker, 1979; Naito and Parker, 2019; Wickert and Schildgen, 2019). This furthermore makes the approach here amenable to straightforward field or remotely sensed observations of channel width and bank height.

In such a rectangular channel, hydraulic radius is defined as:

$$R_h = \frac{bh}{b + 2(h \wedge h_\beta)}. \tag{3}$$

Here, b is channel width, h is flow depth, and h_β is the height of the channel banks. $\wedge$ indicates that the smaller of the two numbers be taken. Therefore, the wetted permieter is computed using the flow depth when the water level lies below the height of the banks, and by the bank height when it is at or above these. Flows that overtop the banks no longer have lateral confinement, and therefore do not encounter additional lateral boundaries in their wetted perimeter.

Assuming that flows deeper than the channel do not experience additional roughness requires that there be no interaction between the floodplain and the flow atop the channel. This assumption is reasonable so long as the channel is much wider than the overbank flows are deep: In this case, most of the flow through the channel will have little effective contact with the no-slip boundary of the floodplain surface. Most natural channels and floods satisfy this criterion (cf. Dunne and Jerolmack, 2020, for a discussion of channel aspect ratios). Therefore, we include flows above the channel within Q_{ch}, the channel component of the discharge.

Flow depth, h, relates to stage as:

$$h = z_s - z_b. \tag{4}$$

Here, we assume that z_b corresponds to the elevation of the channel bed. This, then, sets the point at which discharge equals 0.

https://doi.org/10.5194/egusphere-2023-3118
Preprint. Discussion started: 8 January 2024

Following this rectangular channel approximation, we multiply in-channel velocity by channel cross-sectional area to compute discharge:

$$Q_{\mathrm{ch}} = \bar{u} b h. \tag{5}$$

Expanding the internal variables except for h and R_h provides

$$Q_{\mathrm{ch}} = \frac{b}{n_{\mathrm{ch}}} h R_h^{2/3} S^{1/2}, \tag{6}$$

which expresses the rectangular channel approximation.

2.1.1 Wide-channel approximation

Optionally, one may use the double-Manning approach with the wide-channel approximation – that is, that $b \gg h_\beta$ and therefore $h \approx R_h$ across all flow depths. Under this simplification,

$$Q_{\mathrm{ch}} = \frac{b}{n_{\mathbf{ch}}} h^{5/3} S^{1/2}. \tag{7}$$

In the remainder of this paper, we use Equation 6 for its better representation of the physical system and appropriateness across a wider range of river geometries.

2.2 Floodplain

Flow across floodplains requires a separate but related mathematical expression. Once water enters the floodplain, it interacts with different roughness elements. Furthermore, because the floodplain is a complex surface that varies in elevation, increasing water depths will correspond to increasing widths.

In order to represent the complexity of floodplain flow in a simple mathematical form, we abstract the Manning (1891) equation into a generic power law that includes a roughness term, k_{fp}, and an exponent that relates to floodplain topography as well as any systematic spatial variability within the roughness structure, P_{fp}:

$$Q_{\mathrm{fp}} = k_{\mathrm{fp}} \left(h - h_\beta\right)^{P_{\mathrm{fp}}}. \tag{8}$$

Here we use depth instead of hydraulic radius under the assumption that flows across the floodplain are much wider than they are deep.

We justify this power law using similar hydraulic arguments to those for a standard power-law rating curve, (e.g., Petersen-Øverleir, 2005). Namely, we posit that inundation width and depth distribution can also be described with power-law functions. When combined with Manning's equation, these produce a generalized geometry-times-velocity power-law relationship for discharge.

https://doi.org/10.5194/egusphere-2023-3118
Preprint. Discussion started: 8 January 2024

2.2.1 Explicit Manning's equation for the floodplain

In the simplified case in which the floodplain may be approximated to have a rectangular form that is much wider than it is deep, one could rewrite Equation 8 as

$$Q_{\mathrm{fp}} = \frac{(B-b)}{n_{\mathrm{fp}}} (h - h_\beta)^{5/3} S^{1/2}. \tag{9}$$

Here, B is the width of the valley bottom – that is, the combined floodplain and channel. In this case,

$$k_{\mathrm{fp}} = \frac{(B-b)S^{1/2}}{n_{\mathrm{fp}}}. \tag{10}$$

The wide-floodplain approximation applied here may not always be appropriate: some rivers have floodplains that are only a few channel widths wide. However, many floodplains contain such significant internal roughness (e.g., from vegetation) that the additional drag against their side walls is small in comparison. Therefore, we consider the simplifying wide-floodplain approximation to be reasonable even when not formally defensible based on Equation 3 alone. This use of Manning's equation for the floodplain in addition to the channel prompted our use of "double-Manning" to refer to our approach, even though our more general formulation includes a less-constrained power law for floodplain flow.

2.3 Full equation

We combine Equations 6 and 8 into two cases: flow in the channel, and flow in (and above) the channel and across the floodplain.

$$Q = \begin{cases} Q_{\mathrm{ch}} & \text{if } h \le h_\beta \\ Q_{\mathrm{ch}} + Q_{\mathrm{fp}} & \text{otherwise.} \end{cases} \tag{11}$$

Q_{ch} and Q_{fp} are laterally, rather than vertically, defined. Q_{ch} includes flow both within and above the channel, and Q_{fp} represents only those flows that cover the floodplains (Figure 1).

3 Data constraints

We formulated the double-Manning approach to have parameters whose values are straightforward and/or easy to measure. Defining parameters from field data reduces the remaining uncertainty in the rating curve. Conersely, observing the parameter but allowing it to vary permits the inversion results (Section 4.2) to be checked against the data-based expected value. Such field-data connections ensure that the double-Manning approach can build rating curves by incorporating more than just the stage–discharge data, which can require substantial effort to acquire.

3.1 Field observations

Table 1 holds the parameters alongside information on observation methods and difficulty. This "difficulty" reflects three factors. The first is the ease (including the time required) to make the measurement itself. Stretching a measuring tape across a

https://doi.org/10.5194/egusphere-2023-3118
Preprint. Discussion started: 8 January 2024

Table 1. Parameters for the double-Manning approach and their connection to observations that are independent of stage–discharge data. Observation (Obs.) difficulty qualitatively integrates the difficulty of the measurement, the logistics involved in making it, and how directly what is measured yields a quality estimate for the desired parameter.

Parameter	Variable	Observation method(s)	Obs. difficulty
Channel width [m]	b	Overhead photos, DEMs[a], and/or field surveys	Very Easy
Channel slope	S	DEMs[a], possibly aided by overhead photos, or field surveys	Easy
Channel depth (bank height) [m]	h_β	Gauge-survey data, DEMs, field surveys	Easy
Stage Offset: Stage at Q = 0 [m]	z_b	Approximate mean bed elevation from field surveys	Easy
Manning's n	n	Grain size; Manning's n tables or photos	Intermediate
Floodplain discharge coefficient	k_{fp}	Insight from field surveys or Manning's n tables or photos	Hard
Floodplain discharge exponent	P_{fp}	Insight from topographic and roughness surveys of floodplain	Hard

[a] Digital elevation models

streambank would be easy, wading in a river to measure velocity would be a bit more difficult, and (due to the time required) surveying all floodplain vegetation for stem density (to parameterize roughness) would be much harder. The second factor relates to logistics: it is easier to make an observation from remotely sensed data or archived gauging station notes than it is to go to the field. The third factor indicates how directly the variable in question may be measured. Geometric and velocity data are measured directly as such, whereas estimates of in-channel Manning's n might be obtained via calculations or inferences from gravel grain size, bedforms, and/or woody debris. Floodplain parameters may be even harder to directly estimate, as they relate to flow paths and vegetation distributions. These, therefore, may be easier to back-calculate from stage–discharge data (e.g., Section 5.1).

Measurements of channel width and bank height (i.e., channel depth) link to discharge through the rectangular channel approximation. Therefore, the approximate "rectangular-channel" values for both width and depth should be selected with flow mechanics in mind (e.g., Naito and Parker, 2019). For shallow but wide flows, $Q \propto h^{5/3}$. Because of this exponent, the discharge difference between a shallow flow and no flow can be much less than that between the same shallow flow and a flow of twice its depth. Therefore, channel width should be estimated above low-lying bars, as their inundation will occur with only a small change in discharge. Meanwhile, bank height should be approximated by differencing a characteristic average channel depth that lies between these bars and the thalweg from the elevation of the top of the banks.

3.2 Sensitivity

Equations 6 and 8 inform which observations most significantly constrain the double-Manning solution. Equations 9 and 10 provide additional context when the rectangular floodplain approximation (Section 2.2.1) may be reasonably applied.

The ratio between channel width (b) and Manning's n (Equation 6) indicates that, despite some influence from R_h, these two terms may be nearly free to co-vary. Fortunately, b is the easiest variable to measure, and this often can be done without

https://doi.org/10.5194/egusphere-2023-3118
Preprint. Discussion started: 8 January 2024

field work (Table 1). Some care must be taken to ensure that the width of the approximately rectangular channel is made, rather than the width of the flow at the time of the observation.

3.3 Estimating Manning's n

For additional constraint, Manning's n may be estimated from field data. In sand-bed rivers, Manning's n commonly varies within the range ∼0.018–0.040 (Simons et al., 2004). Hey (1979), followed by a further analysis by Clifford et al. (1992), demonstrated that for gravel-bed rivers, the Nikuradse (1933) roughness parameter $k_s \approx 3.5D_{84}$, where D_{84} is the 84th percentile of the grain-size distribution. Combining the work of Parker (1991) with the definition of Manning's equation provides an algebraic translation between k_s and Mannning's n:

$$n_{\mathrm{ch}} = \frac{k_s^{1/6}}{g^{1/2}\alpha_r}. \tag{12}$$

Here, g is acceleration due to gravity and α_r is a coefficient that increases as the flow becomes faster for a given k_s. For gravel-bed rivers, Parker (1991) found that $\alpha_r \approx 8.1$. Solving for these constants then yields the simple equation relating our two measures of roughness, $n \approx k_s^{1/6}/25$. Therefore while implying that the appropriate units remain in the equation,

$$n_{\mathrm{ch}} \approx 0.049 D_{84}^{1/6}. \tag{13}$$

3.4 Overbank flows

Estimates of bank height provide an expected flow stage at which the rating curve should "roll over". As flow rises above this stage, it enters the floodplain: at this point, a modest increase in stage may require a large increase in discharge. The double-Manning formulation explicitly incorporates this rating-curve feature via overbank flows. Although bank height may be solved for as a free parameter using a large amount of stage–discharge data (Section 5.1), situations involving sparse (or no) data are aided by (or require) independent estimates of bank height (Sections 5.2 and 5.3).

If floodplain geometry and roughness variability be unknown, then P_{fp} and k_{fp} must be left to calibration. To aid parameter estimation, we turn to features of floodplain topography. Floodplains have generally concave-up forms, from flat regions near the river that rise to terraces or valley walls farther from the channel. Such floodplain forms produce greater flow widths – and therefore discharge – as stage increases. Although river levees and abandoned bars do comprise local convexities (e.g., Moody et al., 1999; Hassenruck-Gudipati et al., 2022), these in fact amplify the overall trend towards wider flow occupation as water rises. Therefore, $P_{\mathrm{fp}} = 5/3$, corresponding to a rectangular floodplain cross-sectional geometry, provides a reasonable lower bound for the floodplain-flow exponent. Finally, if the flow-width vs. roughness components of P_{fp} may be separated, then the Manning's n component of k_{fp} may be evaluated. Here we do so only for the simple case of an approximately rectangular floodplain (Section 2.2.1).

https://doi.org/10.5194/egusphere-2023-3118
Preprint. Discussion started: 8 January 2024

4 Numerical implementation and inversion

4.1 Model implementation and interface

We implement the above equations into the `doublemanning` software package. This contains two key modules: `doublemanning-fit` computes an optimized parameter set (Table 1) to fit Equation 11 to stage–discharge data. `doublemanning-calc` computes depth or stage as a function of discharge, as well as discharge as a function of depth or stage. The `doublemanning` package is available via GitHub, archived on Zenodo (Wickert, 2023), and may be downloaded using `pip` from PyPI. This `pip`-based install will install command-line interfaces for both `doublemanning-fit` and `doublemanning-calc`.

Users may access both `doublemanning-fit` and `doublemanning-calc` using self-documented command-line interfaces. For `doublemanning-fit`, channel width, depth, and/or slope may be passed directly via the command-line interfacfe. To additionally set bounds on n, k_{fp}, P_{fp}, z_b, h_β, and/or b, a user may format a YAML file following the guide within the double-Manning repository (Wickert, 2023). We recommend working with YAML files, as these give additional control over plotting and allow the inputs and constraints on the fits to be self-documented.

4.2 Inverse modeling: fitting stage–discharge data

We designed the double-Manning approach to permit multiple links with field data while limiting the required parameters to a modest set, most of which can be readily measured (see Ben-Zion, 2017, for a discussion of model explanatory power vs. complexity). Equation 11 involves four field-measurable parameters: channel width, bank height, channel-bed elevation, and Manning's n. It also includes two free parameters, the power-law coefficient and exponent for flows across the floodplain, which relate to floodplain topography and roughness.

The `doublemanning-fit` software module finds an optimized parameter set (see Table 1) to fit Equation 11 to user-provided stage–discharge data. It does so via a nonlinear least-squares approach using the `curve_fit` method within SciPy (Virtanen et al., 2020). Users can specify values for width (b), depth (h), and/or slope (S); they may also specify bounds for Manning's n, the floodplain coefficient (k_{fp}) and/or exponent (P_{fp}), and the offset between flow depth and river stage (z_b). By directly setting (or setting tight bounds for) these parameters, the scientist can impose known constraints on the system. By loosening these, one can find values that are harder to know (e.g., Manning's n or, harder still, the floodplain parameters). One may also loosen the declared bounds on known parameters to test that the `doublemanning-fit` method recovers expected values.

4.3 Forward modeling

The `doublemanning-calc` module uses the output best-fitting parameters from `doublemanning-fit` to convert between water level and discharge. Directly solving Equation 11 provides discharge as a function of water depth. This same solution method provides discharge as a function of stage, following a first-step subtraction of z_b (Equation 4. Using Equation 11 to calculate water depth (h) from discharge (Q) is not as trivial because h cannot be isolated on one side of the equation.

https://doi.org/10.5194/egusphere-2023-3118
Preprint. Discussion started: 8 January 2024

Therefore, we obtain h and (through trivial addition) z_s from Q using the `fsolve` root-finder built into SciPy (Virtanen et al., 2020).

`fsolve` is a Python frontend to the FORTRAN MINPACK library (Moré et al., 1980), which implements Powell's (1970) dog-leg method for iteratively solving non-linear least-squares problems. Powell's dog-leg method works by applying the Gauß–Newton algorithm so long as the solution lies within an imposed "trust region" of permissible parameter values, and otherwise augments this approach with a forward-difference-style gradient descent. .

5 Field Applications

We apply this double-Manning approach to three rivers (Table 2) to demonstrate the double-Manning method's applicability across a wide range of settings and quantites of available data. From largest to smallest, these are the sand-bedded Minnesota River, gravel-bedded Cannon River, and gravel-to-boulder-bedded La Dormida. These rivers span nearly three orders of magnitude in discharge, four orders of magnitude in slope, and three orders of magnitude in bed-material grain size. Each river has a floodplain. The Minnesota and Cannon Rivers (Minnesota, USA) host long-term USGS stream gauges. We analyze a data set from the Minnesota River spanning 1934–2021, providing more-than-ample information for parameter inversion using the double-Manning approach (Jones and Wickert, 2023). For the Cannon River, we limit or use of stage–discharge data to 2002–2012, during which the stage–discharge relationship appears stable (Jones et al., 2023). A consequence of using this shorter and stabler time period is that it includes few points for large floods. Therefore, our goal here is to combine field observations of channel geometry with stage–discharge data to build the best possible rating curve. The dataset from remote and poorly accessible La Dormida in the Ecuadorian Andes includes just 4 discharge measurements (Nelson, 2021; Jacoby et al., 2022; Ng et al., 2023). To demonstrate how extreme data sparsity can be addressed, we leverage additional observational and theoretical (cf. Gioia and Bombardelli, 2001; Bonetti et al., 2017) constraints in order to apply our double-Manning approach to generate a reasonable rating curve.

5.1 Inversion from ample data: Minnesota River

The Minnesota River near Jordan, Minnesota, USA, drains ~42,000 km^2 of formerly glaciated topography stretching from the eastern portions of the Great Plains to the western edge of the hardwood forests. It meanders across the floor of a valley formed by the Glacial River Warren (cf. Gran et al., 2013). As a major waterway across a now-agricultural post-glacial landscape, the Minnesota River has been gauged at Jordan since 1934. The combined effects of climate change and agricultural expansion, with associated land drainage, caused (and continues to cause) significant channel widening via rapid delivery of water to the river, resulting in larger floods (Engstrom et al., 2009; Blumentritt et al., 2013; Schottler et al., 2014; Lauer et al., 2017; Kelly, 2019). This has required repeated shifts of the Minnesota River's rating curve since the beginning of gauging in order to maintain its ability to predict modern stage–discharge relationships. These shifts ensure that the data points relating to stage and discharge correspond to the modern hydraulic geometry.

https://doi.org/10.5194/egusphere-2023-3118
Preprint. Discussion started: 8 January 2024

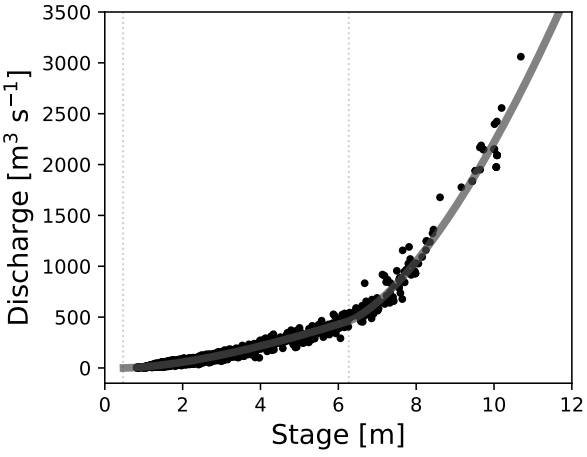

Figure 2. Stage–discharge rating curve for the Minnesota River near Jordan. Field measurements of paired stage and discharge appear as black points, and the rating-curve fit overlies them as a semi-transparent gray line. The light gray dotted lines represent (left) the stage at which discharge is 0 – i.e., z_b, the parameterized channel-bed elevation – and (right) the bankfull stage at $z_b + h_\beta$. Only nuanced visible differences exist between this best-fitting plot, corresponding to the parameters given in Table 1, and a fit in which we force $P_{\mathrm{fp}} = 5/3$ to calculate a floodplain Manning's n. The `doublemanning-fit` software automatically generated this plot and the others like it in this article.

The 1131 shift-adjusted stage–discharge measurement pairs permit us to apply the double-Manning approach with few constraints from data beyond the stage–discharge points. We prescribe modern river width at 100 m and slope at 10^{-4} (Libby, 2018; Minnesota Department of Natural Resources, 2014). We prescribe width at a set value because it is easy to observe and co-varies with Manning's n, which is more difficult to observe (Section 3.2). Manning's n varies between 0.03 and 0.055 at Chaska (U.S. Army Corps of Engineers, 1952), ∼12 km downvalley of the Jordan gauging station. To ensure that we do not overconstrain the problem, we extend our Manning's n search range to 0.25–0.60. We permit channel depth to vary from 4–10 m (Kelly, 2019) and leave k_{fp} and P_{fp} effectively unconstrained.

The solved parameters (Table 1) lie within expectations, and the plotted fit (Figure 2) visually appears accurate; see Table 2 for the root-mean-square error, RMSE). n_{ch} falls within the Chaska data range (U.S. Army Corps of Engineers, 1952), as well as within the n =0.020–0.040 range expected for sand-bed rivers with dune-covered beds (Simons et al., 2004). Channel depth (h_β) is a little less than our field-estimated ∼7 m, but remains close at 5.8 m.

The best-fit $P_{\mathrm{fp}} = 1.62$ is close to $5/3$, which would be expected for a simple full-floodplain inundation without complex topography or roughness structure. We term this the "rectangular floodplain approximation" in Section 2.2.1, above. Such a result is sensible for the Minnesota River, whose steep valley walls (a result of deglacial-megaflood incision: cf. Belmont et al., 2011) confine a broad and essentially flat floodplain.

https://doi.org/10.5194/egusphere-2023-3118
Preprint. Discussion started: 8 January 2024

Noting that P_{fp} corresponds to a near-rectangular floodplain and incorporating our knowledge of valley-bottom width (Table 2), we back-calculate an expected floodplain pseudo-Manning's n from Equation 10 to be 0.072. We refer to this value as a "pseudo-Manning's n" because we compute it with the best-fit k_{fp} from when $P_{\mathrm{fp}} \neq 5/3$. Re-running the inversion problem and holding P_{fp} at $5/3$ results in $k_{\mathrm{fp}} = 126$ and a value of 0.079 for Manning's n itself. Here, floodplains of the Minnesota River comprise forests, fields, and wetlands. Acrement and Schneider (1989) provides Manning's n values of 0.10–0.15 for similarly forested floodplains. Phillips and Tadayon (2006) notes that Manning's n ranges from 0.025–0.050 across floodplain pastures. For submerged vegetation, which we take to be representative of wetlands, Manning's $n < 0.025$ (Phillips and Tadayon, 2006). These values bracket our computed Manning's n on this mixed-land-cover floodplain and provide some confidence in our results.

Taken together, fitting this Minnesota River stage–discharge data set (Jones and Wickert, 2023) demonstrates two concepts to carry forward. First, *a priori* knowledge of floodplain geometry and/or roughness may aid in pre-specifying k_{fp} and/or P_{fp}, thereby further constraining special cases of the the stage–discharge problem. Second, the 2.3× difference between n_{ch} and n_{fp} indicates the importance of explicitly resolving channel–floodplain differences within the rating-curve fit. In a typical power-law rating-curve approach (Eq. 1), such a sudden change in the coefficient may be absorbed by the exponent. This may not be able to match the bend in the stage–discharge curve associated with a transition to floodplain flow. Furthermore, it will not as effectively encapsulate a physically based parameterization of flow processes (cf. Gioia and Bombardelli, 2001; Bonetti et al., 2017), thereby making the meaning behind the values of the rating-curve coefficient and exponent harder to interpret. In contrast, the double-Manning approach permits intuitive adjustments if hydraulic geometry and/or roughness change.

5.2 Fitting more limited data: Cannon River

The Cannon River in southeastern Minnesota, USA, drains 3470 km^2 of woodlands, farms, cities, and forests en route to the Mississippi River valley. Its tributaries cross low-relief uplands, the large western portion of which were ice-covered at the Last Glacial Maximum (Patterson and Hobbs, 1995). Its primary gauge, at the town of Welch, records streamflow within the bedrock-walled and gravel-bedded lower valley of the Cannon River.

When plotting the USGS record of Cannon-river stage and discharge, we noted systematic sub-parallel trends, prominent at low-magnitude discharges, that vanished when we examined a shorter time window. These likely indicate changes in channel hydraulic geometry that were not fully corrected by shift adjustments to the rating-curve data, as they were for the Minnesota River data set, above. As a result, we generate a rating curve appropriate for a subset of data obtained from 2002–2012. This real scenario requires us to reduce the data used, and therefore illustrates how the double-Manning approach may help to fill in gaps within the resultant sparser data set.

As input to `doublemanning-fit`, we measured the hydraulic geometry of the Cannon River (Table 1). Using overhead imagery via Google Earth from the 2002–2012 period, we estimated channel width at the Welch gauge. We computed the slope of the Cannon River from the site of the gauge at Welch to the mouth of Belle Creek, ∼3.5 km downstream, using elevation differences from the Minnesota statewide lidar digital elevation model (DEM) collected in 2011 (Minnesota Department of Natural Resources, 2014). To estimate bank height (h_β), we found and then combined floodplain-surface elevation

https://doi.org/10.5194/egusphere-2023-3118
Preprint. Discussion started: 8 January 2024

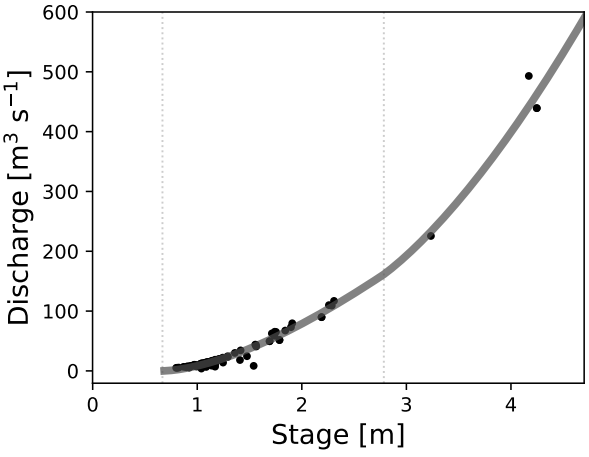

Figure 3. Stage–discharge rating curve for the Cannon River at Welch. Though only few data points constrain the bankfull height of the channel, we used the surveyed stream-gauge elevation alongside lidar topographic data and (iteratively) the computed stage offset to constrain our h_β search window to 2.17±0.33 m.

with channel-bed elevation. We obtained floodplain-surface elevation (Z_{fp}, with the capital Z indicating that this is absolute elevation above sea level) from the Minnesota statewide lidar DEM, with an approximate absolute accuracy of ±0.15 m. We observed the spatial variability in floodplain-surface elevation to be approximately ±0.15 m. To find the channel-bed elevation, we first obtained the surveyed gauge elevation (Z_g, accurate to ±0.03 m). Noting that

$$h_\beta = Z_{\mathrm{fp}} - (Z_g + z_b), \tag{14}$$

the final task is to find the stage offset. We do this by initially guessing that $h_\beta = Z_{\mathrm{fp}} - Z_g$, computing z_b through `doublemanning-fit`, and then updating h_β using Equation 14. Only one iteration was needed to demonstrate that $h_\beta \approx 2.17$ m, thus demonstrating the insensitivity of the in-channel portion of the fit to overbank flows and floodplain processes. We combined this h_β estimate with a sum of the error estimates to constrain h_β within the range of 2.17±0.33 m, which we input to `doublemanning-fit` via its YAML file as our initial parameter estimate (Jones et al., 2023).

The data set contains only three observations of overbank flows, and these constrain k_{fp} and P_{fp} only loosely. Because two of these data points lie close to one another, the data emulate a scenario with two data points, thereby allowing k_{fp} and P_{fp} to trade off against one another in a wide range of parameter pairs that fit the data. This motivates an additional external constraint to reduce the free-parameter space. Here, we follow our prior advice (Section 3) and set the minimum likely value for P_{fp} at 5/3.

We then computed the Cannon River stage–discharge rating curve from its 2002–2012 data set (Figure 3) Our inversion solution returns $P_{\mathrm{fp}} = 5/3$, its prescribed minimum value. We typically would consider this to be a poor result, but here simply accept this based on the lack of available data alongside the good visual and quantitative fit (Figure 3).

https://doi.org/10.5194/egusphere-2023-3118
Preprint. Discussion started: 8 January 2024

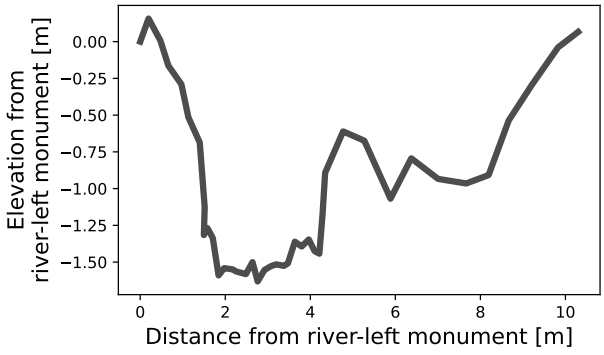

Figure 4. Surveyed cross section elevation profile across La Dormida at the Captación gauging site (Ng et al., 2023). The cross section is plotted from river left to river right (i.e., looking downstream). The approximately rectangular channel on valley left is inset into a roughly rectangular floodplain. The floodplain channel on valley right helps to define the bankfull depth.

As independent control on channel roughness, and hence, Manning's n, we used grain-size data obtained near the Welch gauge (Jones et al., 2023). $D_{84} = 55$ mm (Table 2), corresponding to a Manning's n value of 0.030 (Equation 13). Based on access limitations, these data were gathered upstream of the gauge, at the confluence with a steeper tributary. Therefore, they represent a likely upper bound on the grain-induced in-channel roughness. Our inversion-estimated $n_{\mathrm{ch}} = 0.025$, consistent with this bound placed on it from grain-size observations.

Because $P_{\mathrm{fp}} = 5/3$, we once more can compute n_{fp}. The surrounding landscape comprises farmland and scattered forests. Expected Manning's n values for agricultural fields range from 0.03 (bare) to 0.05 (mature crops) (Phillips and Tadayon, 2006). Those for roughly similar forests in Mississippi, USA, range from 0.10–0.18. Solving Equation 10, we find that $n_{\mathrm{fp}} = 0.061$, which lies between the values for the two land-use types.

Analyzing the Cannon River data set teaches us two lessons. First, field-based parameter estimates – in this case, relating to channel depth and Manning's n – can help to constrain and validate rating-curve parameters. Second, realistic physical bounds on floodplain hypsometry – and hence, P_{fp} – may be required where data are sparse. Both this example and that from the Minnesota River demonstrate that a rectangular floodplain approximation could apply generally.

5.3 Fitting and extrapolating: La Dormida

The La Dormida River originates at the tongue of the Glaciar Hermoso and drains a narrow down-ice watershed on the southwestern flank of Volcán Cayambe, Ecuador. Streamflow in La Dormida comes from a combination of glacier melt, precipitation, and groundwater (including localized hydrothermal) springs (cf. Nelson, 2021). The stream gauge at La Dormida Captación, near the location where the stream starts to leave the mountain, comprises a pressure transducer in a stilling well and a mounted staff gauge (Ng et al., 2023). At the gauging site, La Dormida has an extremely steep cobble- to boulder-bed channel: a typical gravel-bed channel has a slope near 0.01, whereas for La Dormida Captación, $S = 0.0788$. Because of its remote location and

https://doi.org/10.5194/egusphere-2023-3118
Preprint. Discussion started: 8 January 2024

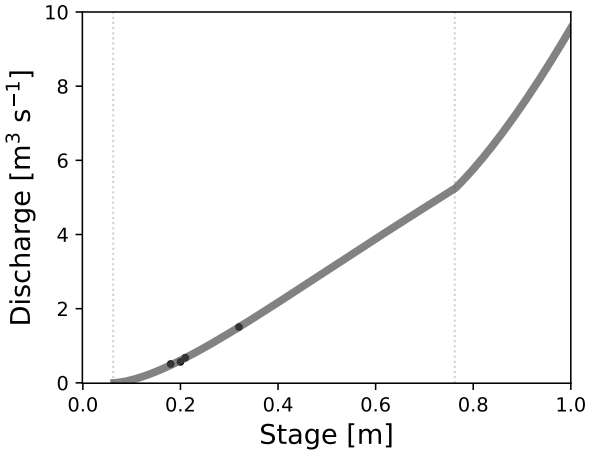

Figure 5. Stage–discharge rating curve for La Dormida Captación.

development as part of a water-resources research project, only four paired stage–discharge measurements have been made, none of which incorporate overbank flow.

A surveyed cross section at La Dormida Captación (Figure 4) presents an approximately rectangular river channel. This shape validates our rectangular channel approximation for the in-channel portion of this double-Manning approach. Critically, it also gives us an approximation of $h_\beta = 0.7$ m, which we base on the vertical distance between the channel bed and a height $\sim$10 cm above the surveyed floodplain channel but significantly below the natural levee. This narrow and steep-walled channel also presents a case in which using the hydraulic radius produces a significantly more accurate solution than using the depth via the wide-channel approximation (Equation 7).

Although floodplain topography is more complex than that of the channel, we also approximate its hydraulic geometry to be rectangular. This rectangular floodplain approximation enables us to apply Equation 9, which fixes $P_{\mathrm{fp}} = 5/3$, and extrapolate the rating curve by approximating n_{fp}. Near the gauge, floodplain vegetation comprises dense forest, tussock grasses, and small open spaces. By visually comparing floodplain-vegetation character and density to the reference sites from Acrement and Schneider (1989), we assign $n_{\mathrm{fp}} = 0.14$. Combining this with our estimated valley-bottom width (Figure 4), we use Equation 10 to solve for k_{fp}. We justify using the wide-floodplain approximation, despite the possibility of a flow width-to-depth ratio below 10, because the Manning's n is large compared to the impact of side-wall drag.

To augment the few stage–discharge data points, we constrained roughness by measuring the in-channel grain-size distribution (Table 2). From the measured $D_{84} = 180$ mm, we compute $n_{\mathrm{ch}} = 0.037$. We could impose this on the fit, but instead allow n_{ch} to remain a free parameter whose value we then evaluate against this expectation.

We inverted these limited stage–discharge data – alongside the aforementioned constraints on channel geometry, floodplain width, and floodplain roughness – to obtain a best-fitting stage–discharge curve (Figure 5). The estimated $n_{\mathrm{ch}} = 0.38$, which is virtually identical to the $n_{\mathrm{ch}} = 0.37$ value estimated from grain size (Table 2). Although the stage–discharge relationship

https://doi.org/10.5194/egusphere-2023-3118
Preprint. Discussion started: 8 January 2024

for overbank flows remains unconstrained by stage–discharge data, the surveyed hydraulic geometry (Figure 4) and land-cover character provide a physically based first estimate for this portion of the rating curve.

6 Discussion

The physical basis of the double-Manning approach offers three notable benefits for establishing river stage–discharge relationships. First, it explicitly distinguishes in-channel and overbank flow, providing the expected inflection in the rating curve when flows overtop the channel margins. Second, it permits links to and tests against field data that (a) augment the standard paired stage–discharge measurements and (b) in many cases are easier to measure. Third, many of these physically based parameters may continue to be used following changes in hydraulic geometry, which may occur due to individual floods (Hofmeister et al., 2023) or in response to progressive changes in hydrological forcings as climate and land use change (Schottler et al., 2014). We then discuss how this flexibility may enable us to simulate the hydrogeomoprphic coupling among changing hydraulic geometry, discharge, and shear stress.

6.1 Explicit overbank region

Most rivers on Earth self-organize into either a channel and floodplain or – in the case of rapidly incising streams – a channel surrounded by valley walls of a different geometry (Pfeiffer et al., 2017; Naito and Parker, 2019; Turowski et al., 2023). The double-Manning approach acknowledges the natural break that occurs between the in- and beyond-channel regions. This allows physically meaningful parameters regarding the shape and roughness of these regions.

Making this overbank region and its associated parameters explicit and distinct enables the other two noted advantages of the double-Manning approach. First, it permits direct comparison against and/or guidance from field data, which naturally vary across geomorphic process-domain boundaries (i.e.: channel to floodplain or hillslope: Section 3; Table 1). Second, it separates the effects of channel–overbank-region (often, channel–floodplain) form from the power-law exponent (Equation 1) and unmixes channel and overbank-region flow resistance. Therefore, we distinguish roughness and geometric parameters from one another, and can, for example, solve for evolving hydraulic geometry using known roughness values.

6.2 Model suitability

We constructed the double-Manning model to streamline rating-curve development for the user while making the underlying hydraulics better represent those of a river. We hope that the former enables straightforward uptake of the double-Manning approach, including further implementation and tests of its usefulness. We expect that the latter will improve data–model integration and the predictive capacity of stage–discharge rating curves, including extrapolation to changing hydraulic geometry and/or roughness (Sections 6.3 and 6.4).

Although the double-Manning formulation involves seven parameters (Table 1) – many more than the three employed by the standard power-law fit (Equation 1) – we argue that it more tightly constrains the physical system and therefore is a more effective model. Whereas the parameters in the power-law fit are empirically determined, the double-Manning approach

https://doi.org/10.5194/egusphere-2023-3118
Preprint. Discussion started: 8 January 2024

separates the constituents of these lumped parameters into physically based and understandable terms. Through this, it brings multiple additional and often easily measurable pieces of information to bear on the problem of relating river discharge to water level, thereby enhancing our ability to develop rating curves.

The two least-measurable terms within the double-Manning formulation are k_{fp} and P_{fp}. However, these retain more physical meaning than the corresponding k and P of the traditional power-law fit (Equation 1) because they apply only to flows across the floodplain. This floodplain-only definitions bounds likely values for P_{fp}. Indeed, our examples (Section 5) demonstrate that floodplain geometry may be approximately rectangular, yielding $P_{\mathrm{fp}} = 5/3$ and an easily defined true "double-Manning" expression. In this case, k_{fp} scales inversely with n_{fp} (Equation 8), itself estimatable through field observations (cf. Acrement and Schneider, 1989).

The simplicity but physical basis of the double-Manning approach, combined with its ready-to-use numerical implementation (Wickert, 2023), establish it as "useful". On one side of it lie distributed hydraulic models (e.g., Kean and Smith, 2005; McDonald et al., 2005; Quintero et al., 2021), which are accurate but take work and expertise to apply, and therefore are not part of the common approach to developing rating curves (cf. World Meteorological Organization, 2010b). To the other side lies the straightforward power law in Equation 1, which may easily be fit to data, but which lacks extrapolatability and may connect only indirectly to our physical understanding of flow processes (Petersen-Øverleir, 2005). Therefore, we hope for the double-Manning approach to be an immediate and ready-to-use upgrade for operational river monitoring and prediction efforts.

6.3 Flexible rating curves

Traditional rating curves are often "shift-adjusted" to incorporate changes in hydraulic geometry that affect the stage–discharge relationship between one measuring time and another (Mansanarez et al., 2019a; Hofmeister et al., 2023). However, such shift adjustments come with three key complexities. First, they are empirically determined and therefore require resurveying the channel cross section and making additional streamflow measurements. While obtaining more data is always helpful, sometimes the act of obtaining these data is not convenient. Second, these shifts are most commonly accomplished by changing z_b in Equation 1. However, it may be the channel width rather than the bed elevation that changes, which should affect the power-law stage–discharge relationship instead of simply the stage offset. Third, alterations to Equation 1 lack straightforward relation to measureable quantities, therefore rendering it brittle – that is, prone to failure – in the face of change and requiring significant effort to resurvey and establish an updated rating curve.

The double-Manning approach provides a flexible alternative to this unadaptable standard method. Users of the double-Manning approach may, for example, change bank height or width while maintaining other parameters. This can allow a rating curve to be updated dynamically based on remotely observed changes in channel width, for example, and permits the calibrated Manning's n and floodplain parameters to be used despite changing hydraulic geometry. This may further extend rating-curve utility, especially in data-sparse settings (Birgand et al., 2013; Nelson, 2021).

https://doi.org/10.5194/egusphere-2023-3118
Preprint. Discussion started: 8 January 2024

6.4 Hydrogeomorphic feedbacks

The double-Manning approach's flexible adaptation to changing hydraulic geometry offers a crucial advantage for research into fluvial geomorphology, which may feed back into improved predictions of stage–discharge relationships in hydrology. Under steady and uniform flow conditions, increased discharge yields deeper water, which exerts higher shear stresses against the channel bed and banks. If these stresses exceed those required to mobilize sediment or erode cohesive material, the channel may increase and/or decrease in size via erosion and/or deposition. Such changes may alter z_b, h_β, and b; changes to n_{ch} and S are also possible, but we neglect these here because the former requires knowledge of sediment sources and the latter changes over (typically) hundreds to thousands of years (Naito and Parker, 2019; Wickert and Schildgen, 2019; Naito and Parker, 2020).

Changing channel geometry undermines key simplifying assumptions in stage–discharge relationships. The traditional power-law rating curve permits data to be "shift-adjusted" via offsets from a standard z_b given to individual data points. However, because it lacks other degrees of freedom, these shift adjustments may also be used to emulate changes in channel width or bankfull channel depth – due, for example, to channel widening or an increase in floodplain height via floodplain deposition. However, each of these changes affects the shape of the rating curve and not just its 0-offset location. In contrast, the double-Manning approach allows these variables to be controlled independently and accounts for their dynamics.

Better understanding such changes to channel hydraulic geometry may enable applications within and beyond rating-curve development. Geomorphologists commonly consider a single "channel-forming discharge" to set river hydraulic geometry (e.g., Copeland et al., 2012; Wickert and Schildgen, 2019). Transient geomorphic evolution feeds back into flow and shear-stress distributions that further shape the channel and alter its streamflow rating curve. Such changes impact flood-hazard potential by altering river-channel conveyance capacity (e.g., Slater et al., 2015; Slater, 2016; Blom et al., 2017; Slater et al., 2019; Wood, 2023). They also make it difficult to know when a rating curve should be shifted (Hofmeister et al., 2023). This combination of physical coupling and practical impact serves to motivate continuing work to generate coupled hydrogeomorphic predictions, which the double-Manning approach makes possible.

7 Conclusions

We offer the double-Manning approach as a step upgrade from the standard power-law equation for generating stage–discharge rating curves. The double-Manning approach incorporates key components of channel and floodplain geometry alongside basic mechanics of steady, uniform, open-channel flow. This additional physical realism comes with no added end-user complexity: the `doublemanning` package generates straightforward curve fits to measured stage–discharge data, which may be further informed by field and remotely sensed observations of the channel and floodplain. By replacing lumped parameters with physically based ones, the double-Manning approach enables flexible and physically meaningful adjustments as hydraulic geometry evolves. In three examples, we demonstrated how double-Manning inverse-model solutions can be tested against or informed by field observations, as well as how the double-Manning approach may provide physically based extrapolations, useful when establishing short-term gauging stations in remote settings.

https://doi.org/10.5194/egusphere-2023-3118
Preprint. Discussion started: 8 January 2024

Code and data availability. The `doublemanning` software package is available via GitHub (github.com/MNiMORPH/doublemanning) and archived through Zenodo (Wickert, 2023). It may be installed from PyPI using `pip`: https://pypi.org/project/doublemanning/. Data sets and associated double-Manning files may be downloaded from GitHub and Zenodo as follows: Minnesota River near Jordan – https://github.com/MNiMORPH/stage-discharge_Minnesota-Jordan (Jones and Wickert, 2023); Cannon River at Welch – https://github.com/MNiMORPH/stage-discharge_Cannon-Welch (Jones et al., 2023); La Dormida Captación – https://github.com/MNiMORPH/stage-discharge_LaDormida-Captacion (Ng et al., 2023).

Author contributions. AW developed the idea, wrote the code, computed the rating curves, and wrote the manuscript. JCJ assembled data for the Minnesota and Cannon Rivers, discussed the ideas, and edited the manuscript. GCN installed and managed the La Dormida stream gauge (including roughness and cross-sectional surveys), discussed the ideas and their implementation, and edited the manuscript.

Competing interests. The authors have no competing financial interests.

Acknowledgements. Campbell Dunn wrote an early version of the command-line interface for `doublemanning-fit`. Daniel Stanton, Jeff La Frenierre, Shauna Capron, Leah Nelson, and Ally Jacoby monitored and maintained the stream gauge at La Dormida Captación. The USGS freely provides stream-gauge data for the Minnesota and Cannon Rivers. Kaya Koraleski, Jake Benbow, and Emma Johnson measured bed-material grain size near the Welch gauge on the Cannon River. This material is based upon work supported by the National Science Foundation under Grants No. 1758795 and 1944782. ADW additionally received support through a Humboldt-Forschungsstipendium from the Alexander von Humboldt-Stiftung.

https://doi.org/10.5194/egusphere-2023-3118
Preprint. Discussion started: 8 January 2024

References

Abril, J. and Knight, D.: Stage-discharge prediction for rivers in flood applying a depth-averaged model, Journal of Hydraulic Research, 42, 616–629, https://doi.org/10.1080/00221686.2004.9628315, 2004.

Acrement, G. J. and Schneider, V. R.: Guide for Selecting Manning's Roughness Coefficients for Natural Channels and Flood Plains, vol. 2339, United States Government Printing Office, Washington, D.C., https://doi.org/10.3133/wsp2339, publication Title: United States Geological Survey Water-Supply Paper Report No.: FHWA-TS-84-204, 1989.

Ahilan, S., O'Sullivan, J. J., Bruen, M., Brauders, N., and Healy, D.: Bankfull discharge and recurrence intervals in Irish rivers, Proceedings of the Institution of Civil Engineers - Water Management, 166, 381–393, https://doi.org/10.1680/wama.11.00078, 2013.

Baffaut, C., Sudduth, K., and Sadler, E.: Comparisons of radar, bubbler, and float water levels in the Goodwater Creek Experimental Watershed, in: Enhancing Landscapes for Sustainable Intensification and Watershed Resiliency—Proceedings of the Seventh Interagency Conference on Research in the Watersheds, edited by Latimer, J. S., Bosch, D. D., Faustini, J., Lane, C. R., and Trettin, C. C., pp. 99–109, U.S. Department of Agriculture Forest Service, Tifton, GA, USA, 2020.

Belmont, P., Gran, K. B., Schottler, S. P., Wilcock, P. R., Day, S. S., Jennings, C., Lauer, J. W., Viparelli, E., Willenbring, J. K., Engstrom, D. R., and Parker, G.: Large shift in source of fine sediment in the upper Mississippi river., Environmental science & technology, 45, 8804–8810, https://doi.org/10.1021/es2019109, 2011.

Ben-Zion, Y.: On different approaches to modeling, Journal of Geophysical Research: Solid Earth, 122, 558–559, https://doi.org/10.1002/2016JB013922, 2017.

Birgand, F., Lellouche, G., and Appelboom, T.: Measuring flow in non-ideal conditions for short-term projects: Uncertainties associated with the use of stage-discharge rating curves, Journal of Hydrology, 503, 186–195, https://doi.org/10.1016/j.jhydrol.2013.09.007, 2013.

Blom, A., Arkesteijn, L., Chavarrías, V., and Viparelli, E.: The equilibrium alluvial river under variable flow and its channel-forming discharge, Journal of Geophysical Research: Earth Surface, 122, 1924–1948, https://doi.org/10.1002/2017JF004213, 2017.

Blumentritt, D. J., Engstrom, D. R., and Balogh, S. J.: A novel repeat-coring approach to reconstruct recent sediment, phosphorus, and mercury loading from the upper Mississippi River to Lake Pepin, USA, Journal of Paleolimnology, https://doi.org/10.1007/s10933-013-9724-8, 2013.

Bonetti, S., Manoli, G., Manes, C., Porporato, A., and Katul, G. G.: Manning's formula and Strickler's scaling explained by a co-spectral budget model, Journal of Fluid Mechanics, 812, 1189–1212, https://doi.org/10.1017/jfm.2016.863, 2017.

Brunner, G. W.: HEC-RAS River Analysis System: Hydraulic Reference Manual, Version 5.0, vol. CPD-69, US Army Corps of Engineers–Hydrologic Engineering Center, Davis, California, USA, 1995.

Buahin, C. A., Sangwan, N., Fagan, C., Maidment, D. R., Horsburgh, J. S., Nelson, E. J., Merwade, V., and Rae, C.: Probabilistic Flood Inundation Forecasting Using Rating Curve Libraries, JAWRA Journal of the American Water Resources Association, 53, 300–315, https://doi.org/10.1111/1752-1688.12500, 2017.

Clifford, N. J., Robert, A., and Richards, K. S.: Estimation of flow resistance in gravel-bedded rivers: A physical explanation of the multiplier of roughness length, Earth Surface Processes and Landforms, 17, 111–126, https://doi.org/10.1002/esp.3290170202, iSBN: 0197-9337, 1992.

Copeland, R., Soar, P., and Thorne, C.: Channel-Forming Discharge and Hydraulic Geometry Width Predictors in Meandering Sand-Bed Rivers, in: Impacts of Global Climate Change, edited by Walton, R., pp. 1–12, American Society of Civil Engineers, Anchorage, Alaska, United States, https://doi.org/10.1061/40792(173)568, 2012.

https://doi.org/10.5194/egusphere-2023-3118
Preprint. Discussion started: 8 January 2024

Dunne, K. B. and Jerolmack, D. J.: What sets river width?, Science Advances, 6, https://doi.org/10.1126/sciadv.abc1505, 2020.

Engstrom, D. R., Almendinger, J. E., and Wolin, J. A.: Historical changes in sediment and phosphorus loading to the upper Mississippi River: mass-balance reconstructions from the sediments of Lake Pepin, Journal of Paleolimnology, 41, 563–588, https://doi.org/10.1007/s10933-008-9292-5, iSBN: 1093300892, 2009.

Ghadai, M., Satapathi, D. P., and Narashimham, M. L.: International Journal of Advanced Research in Engineering and Technology (IJARET), International Journal of Advanced Research in Engineering and Technology (IJARET), 11, 490–499, 2020.

Gioia, G. and Bombardelli, F. A.: Scaling and Similarity in Rough Channel Flows, Physical Review Letters, 88, 014 501, https://doi.org/10.1103/PhysRevLett.88.014501, publisher: American Physical Society, 2001.

Gran, K. B., Finnegan, N., Johnson, A. L., Belmont, P., Wittkop, C., Rittenour, T., Day, S. S., Jennings, C., Lauer, J. W., Wilcock, P. R., Finnegan, N., Jennings, C., Lauer, J. W., and Wilcock, P. R.: Landscape evolution, valley excavation, and terrace development following abrupt postglacial base-level fall, GSA Today, 125, 1851–1864, https://doi.org/10.1130/G121A.1, 2013.

Hamilton, S., Maynard, R., and Kenney, T.: Comparative Investigation of Canadian, US, and Australian Stage-Discharge Rating Curve Development, in: Australian Hydrographers Association Conference, Canberra, Australia, 2016.

Harpold, A. A., Mostaghimi, S., Vlachos, P. P., Brannan, K., and Dillaha, T.: Stream Discharge Measurement Using a Large-Scale Particle Image Velocimetry (LSPIV) Prototype, Transactions of the ASABE, 49, 1791–1805, https://doi.org/10.13031/2013.22300, 2006.

Hassenruck-Gudipati, H. J., Passalacqua, P., and Mohrig, D.: Natural levees increase in prevalence in the backwater zone: Coastal Trinity River, Texas, USA, Geology, 50, 1068–1072, https://doi.org/10.1130/G50011.1, 2022.

Hey, R. D.: Flow Resistance in Gravel-Bed Rivers, Journal of the Hydraulics Division, 105, 365–379, https://doi.org/10.1061/JYCEAJ.0005178, 1979.

Hofmeister, F., Venegas, B. R., Sentlinger, G., Tarantik, M., Blume, T., Disse, M., and Chiogna, G.: Automated streamflow measurements in high-elevation Alpine catchments, River Research and Applications, n/a, https://doi.org/10.1002/rra.4203, 2023.

Hrafnkelsson, B., Sigurdarson, H., Rögnvaldsson, S., Jansson, A. Ö., Vias, R. D., and Gardarsson, S. M.: Generalization of the power-law rating curve using hydrodynamic theory and Bayesian hierarchical modeling, Environmetrics, 33, e2711, https://doi.org/10.1002/env.2711, 2022.

Hut, R., Drost, N., van de Giesen, N., van Werkhoven, B., Abdollahi, B., Aerts, J., Albers, T., Alidoost, F., Andela, B., Camphuijsen, J., Dzigan, Y., van Haren, R., Hutton, E., Kalverla, P., van Meersbergen, M., van den Oord, G., Pelupessy, I., Smeets, S., Verhoeven, S., de Vos, M., and Weel, B.: The eWaterCycle platform for open and FAIR hydrological collaboration, Geoscientific Model Development, 15, 5371–5390, https://doi.org/10.5194/gmd-15-5371-2022, 2022.

Jacoby, A., Ng, G. H. C., Barker, J. D., La Frenierre, J., Stanton, D., Manciati, C. P., Minaya, V. G., Zapata-Rios, X., and Wickert, A. D.: Investigating Distinct Drivers of Hydrochemical Change Across the Vulnerable Glacierized Tropics, in: AGU Fall Meeting, vol. 2022, pp. H25L–1252, https://ui.adsabs.harvard.edu/abs/2022AGUFM.H25L1252J, conference Name: AGU Fall Meeting Abstracts ADS Bibcode: 2022AGUFM.H25L1252J, 2022.

Jones, J. and Wickert, A. D.: Minnesota River near Jordan: stream-gauge data and double-Manning fit., https://doi.org/10.5281/zenodo.10334289, 2023.

Jones, J., Wickert, A. D., Koraleski, K., Benbow, J., and Johnson, E.: Cannon River at Welch: stream-gauge data (stage, discharge, and sediment grain size) and double-Manning fit., https://doi.org/10.5281/zenodo.10334497, 2023.

Kean, J. W. and Smith, J. D.: Generation and verification of theoretical rating curves in the Whitewater River basin, Kansas, Journal of Geophysical Research, 110, 1–17, https://doi.org/10.1029/2004JF000250, 2005.

https://doi.org/10.5194/egusphere-2023-3118
Preprint. Discussion started: 8 January 2024

Kean, J. W. and Smith, J. D.: Calculation of stage-discharge relations for gravel bedded channels, Journal of Geophysical Research, 115, 1–15, https://doi.org/10.1029/2009JF001398, 2010.

Kelly, S. A.: River Hydrology, Morphology, and Dynamics in an Intensively Managed, Transient Landscape, Ph.D., Utah State University, United States – Utah, https://www.proquest.com/docview/2210132625/abstract/C4896794F5834017PQ/1, iSBN: 9781392049655, 2019.

Kruger, A., Krajewski, W. F., Niemeier, J. J., Ceynar, D. L., and Goska, R.: Bridge-Mounted River Stage Sensors (BMRSS), IEEE Access, 4, 8948–8966, https://doi.org/10.1109/ACCESS.2016.2631172, 2016.

Lauer, J. W., Echterling, C., Lenhart, C., Belmont, P., and Rausch, R.: Air-photo based change in channel width in the Minnesota River basin: Modes of adjustment and implications for sediment budget, Geomorphology, 297, 170–184, https://doi.org/10.1016/j.geomorph.2017.09.005, publisher: Elsevier B.V., 2017.

Leopold, L. B. and Maddock, T.: The hydraulic geometry of stream channels and some physiographic implications, no. 252 in Professional Paper, United States Geological Survey, Washington, D.C., 1953.

Leopold, L. B., Wolman, M. G., and Miller, J. P.: Fluvial processes in geomorphology, W. H. Freeman, San Francisco, CA, USA, https://doi.org/10.1016/0022-1694(65)90101-0, publication Title: Journal of Hydrology ISSN: 00221694, 1964.

Libby, D.: Assessing historical planform channel change in an altered watershed with quantification of error and uncertainty present in a GIS/aerial photography-based analysis; case study: Minnesota River, Minnesota, USA, Ph.D. thesis, Minnesota State University, Mankato, USA, volume: M.S. Issue: May ISSN: 0886-2605, 2018.

Luppi, L., Rinaldi, M., Teruggi, L. B., Darby, S. E., and Nardi, L.: Monitoring and numerical modelling of riverbank erosion processes: a case study along the Cecina River (central Italy), Earth Surface Processes and Landforms, 557, 547–557, https://doi.org/10.1002/esp.1754, 2009.

Manning, R.: On the flow of water in open channels and pipes, Trans. Inst. Civil Eng. Ireland, 20, 1891.

Mansanarez, V., Renard, B., Coz, J. L., Lang, M., and Darienzo, M.: Shift Happens! Adjusting Stage-Discharge Rating Curves to Morphological Changes at Known Times, Water Resources Research, 55, 2876–2899, https://doi.org/10.1029/2018WR023389, 2019a.

Mansanarez, V., Westerberg, I. K., Lam, N., and Lyon, S. W.: Rapid Stage-Discharge Rating Curve Assessment Using Hydraulic Modeling in an Uncertainty Framework, Water Resources Research, 55, 9765–9787, https://doi.org/10.1029/2018WR024176, 2019b.

McDonald, R. R., Nelson, J. M., and Bennett, J. P.: Multi-Dimensional Surface-Water Modeling System User's Guide, vol. 6-B2 of *US Geological Survey Techniques and Methods*, U.S. Geological Survey, 2005.

Minnesota Department of Natural Resources: MnTopo LiDAR Digital Elevation Model, 2014.

Moody, J. A., Pizzuto, J. E., and Meade, R. H.: Ontogeny of a flood plain, GSA Bulletin, 111, 291–303, https://doi.org/10.1130/0016-7606(1999)111<0291:OOAFP>2.3.CO;2, 1999.

Moré, J. J., Garbow, B. S., and Hillstrom, K. E.: User guide for MINPACK-1, vol. ANL-80-74, Argonne National Laboratory, 1980.

Naito, K. and Parker, G.: Can Bankfull Discharge and Bankfull Channel Characteristics of an Alluvial Meandering River be Cospecified From a Flow Duration Curve?, Journal of Geophysical Research: Earth Surface, 124, 2381–2401, https://doi.org/10.1029/2018JF004971, 2019.

Naito, K. and Parker, G.: Adjustment of self-formed bankfull channel geometry of meandering rivers: modelling study, Earth Surface Processes and Landforms, 45, 3313–3322, https://doi.org/10.1002/esp.4966, 2020.

Nelson, L.: Hydrogeochemical characterization of glacierized watersheds in the subhumid inner tropics, Master's thesis, University of Minnesota, Minneapolis, Minnesota, USA, https://hdl.handle.net/11299/224506, 2021.

https://doi.org/10.5194/egusphere-2023-3118
Preprint. Discussion started: 8 January 2024

Ng, G.-H. C., La Frenierre, J., Stanton, D., Wickert, A. D., Nelson, L., Capron, S., and Jacoby, A.: Stream-gauging Data: La Dormida Captación, https://doi.org/10.5281/zenodo.10334038, 2023.

Nikuradse, J.: Strömungsgesetze in Rauhen Rohren, Forschungsheft auf dem Gebiete des Ingenieurwesens, 361, 361, 1933.

Noto, S., Tauro, F., Petroselli, A., Apollonio, C., Botter, G., and Grimaldi, S.: Low-cost stage-camera system for continuous water-level monitoring in ephemeral streams, Hydrological Sciences Journal, 67, 1439–1448, https://doi.org/10.1080/02626667.2022.2079415, 2022.

Parker, G.: Hydraulic geometry of active gravel rivers, Journal of the Hydraulics Division, 105, 1185–1201, iSBN: 0044-796X, 1979.

Parker, G.: Downstream variation of grain size in gravel rivers: Abrasion versus selective sorting, in: Fluvial Hydraulics of Mountain Regions, edited by Armanini, A. and Di Silvio, G., vol. 37, pp. 345–360, Springer, Berlin, Heidelberg, https://doi.org/10.1007/BFb0011201, series Title: Lecture Notes in Earth Sciences, 1991.

Patterson, C. J. and Hobbs, H. C.: Surficial geology, in: County Atlas C-9: Geologic atlas of Rice County, edited by Hobbs, H. C., vol. pl. 3, Minnesota Geological Survey, Saint Paul, Minnesota, USA, series Title: 1:100,000, 1995.

Paul, J. D., Buytaert, W., and Sah, N.: A Technical Evaluation of Lidar-Based Measurement of River Water Levels, Water Resources Research, 56, https://doi.org/10.1029/2019WR026810, 2020.

Petersen-Øverleir, A.: A hydraulics perspective on the power-law stage-discharge rating curve, NVE Report 5-05, Norwegian Water Resources and Energy Directorate, Oslo, Norway, 2005.

Pfeiffer, A. M., Finnegan, N. J., and Willenbring, J. K.: Sediment supply controls equilibrium channel geometry in gravel rivers, Proceedings of the National Academy of Sciences, 114, 201612 907, https://doi.org/10.1073/pnas.1612907114, arXiv: 1408.1149 ISBN: 0711232105, 2017.

Phillips, J. V. and Tadayon, S.: Selection of Manning's Roughness Coefficient for Natural and Constructed Vegetated and Non-Vegetated Channels, and Vegetation Maintenance Plan Guidelines for Vegetated Channels in Central Arizona, Scientific Investigations Report 2006–5108, U.S. Geological Survey, Reston, Virginia, USA, doi: 10.3133/sir20065108, 2006.

Pitlick, J. and Van Steeter, M. M.: Geomorphology and endangered fish habitats of the upper Colorado River: 2. Linking sediment transport to habitat maintenance, Water Resources Research, 34, 303–316, https://doi.org/10.1029/97WR02684, 1998.

Powell, M. J. D.: A hybrid method for nonlinear equations, in: Numerical Methods for Nonlinear Algebraic Equations, edited by Robinowitz, P., pp. 87–144, Gordon and Breach Science, London, https://cir.nii.ac.jp/crid/1571135650078362496, 1970.

Quezada, V. M., Hernández, J.-H., Miranda, R., Padilla, F., Li, Y., Knappett, P., Murrieta, D., Vázquez, A., and Bian, J.: Experimental instrumentation of water stage monitoring stations in mountain streams bedrock using pressure transducers, Flow Measurement and Instrumentation, 93, 102 436, https://doi.org/10.1016/j.flowmeasinst.2023.102436, 2023.

Quintero, F., Rojas, M., Muste, M., Krajewski, W. F., Perez, G., Johnson, S., Anderson, A., Hunemuller, T., Cappuccio, B., and Zogg, J.: Development of Synthetic Rating Curves: Case Study in Iowa, Journal of Hydrologic Engineering, 26, 05020 046, https://doi.org/10.1061/(ASCE)HE.1943-5584.0002022, 2021.

Sauer, V. B. and Turnipseed, D. P.: Stage measurement at gaging stations, Tech. Rep. 3-A7, U.S. Geological Survey, https://doi.org/10.3133/tm3A7, iSSN: 2328-7055 Publication Title: Techniques and Methods, 2010.

Schmidt, A. R. and Yen, B. C.: Theoretical Development of Stage-Discharge Ratings for Subcritical Open-Channel Flows, Journal of Hydraulic Engineering, 134, 1245–1256, https://doi.org/10.1061/(ASCE)0733-9429(2008)134:9(1245), 2008.

Schottler, S. P., Ulrich, J., Belmont, P., Moore, R., Lauer, J. W., Engstrom, D. R., and Almendinger, J. E.: Twentieth century agricultural drainage creates more erosive rivers, Hydrological Processes, 28, 1951–1961, https://doi.org/10.1002/hyp.9738, 2014.

https://doi.org/10.5194/egusphere-2023-3118
Preprint. Discussion started: 8 January 2024

Simons, D. B., Richardson, E. V., Albertson, M. L., and Kodoatie, R. J.: Geomorphic, Hydrologic, Hydraulic, and Sediment Transport Concepts Applied to Alluvial Rivers, Colorado State University, 2004.

Siqueira, V. A., Sorribas, M. V., Bravo, J. M., Collischonn, W., Lisboa, A. M. V., and Trinidad, G. G. V.: Real-time updating of HEC-RAS model for streamflow forecasting using an optimization algorithm, RBRH, 21, 855–870, https://doi.org/10.1590/2318-0331.011616086, 2016.

Slater, B.: Lake projects address locks, dredging, Duluth News Tribune, 2016.

Slater, L. J., Singer, M., and Kirchner, J. W.: Drivers of flood hazard, Geophysical Research Letters, 42, 370–376, https://doi.org/10.1002/2014GL062482, 2015.

Slater, L. J., Khouakhi, A., and Wilby, R. L.: River channel conveyance capacity adjusts to modes of climate variability, Scientific Reports, 9, 1–10, https://doi.org/10.1038/s41598-019-48782-1, 2019.

Somers, L. D., McKenzie, J. M., Zipper, S. C., Mark, B. G., Lagos, P., and Baraer, M.: Does hillslope trenching enhance groundwater recharge and baseflow in the Peruvian Andes?, Hydrological Processes, 32, 318–331, https://doi.org/10.1002/hyp.11423, 2018.

Tauro, F., Petroselli, A., Porfiri, M., Giandomenico, L., Bernardi, G., Mele, F., Spina, D., and Grimaldi, S.: A novel permanent gauge-cam station for surface flow observations on the Tiber river, Geoscientific Instrumentation, Methods and Data Systems Discussions, pp. 1–17, https://doi.org/10.5194/gi-2015-17, 2016.

Turnipseed, D. P. and Sauer, V. B.: Discharge measurements at gaging stations, Tech. Rep. 3-A8, U.S. Geological Survey, https://doi.org/10.3133/tm3A8, iSSN: 2328-7055 Publication Title: Techniques and Methods, 2010.

Turowski, J. M., Bufe, A., and Tofelde, S.: A process-based model for fluvial valley width, EGUsphere [preprint], https://doi.org/10.5194/egusphere-2023-1770, 2023.

U.S. Army Corps of Engineers: Minnesota River at Chaska, Minnesota, vol. Technical Appendices, U.S. Army Corps of Engineers, St. Paul, Minnesota, USA, 1952.

Van Steeter, M. M. and Pitlick, J.: Geomorphology and endangered fish habitats of the upper Colorado River: 1. Historic changes in streamflow, sediment load, and channel morphology, Water Resources Research, 34, 287–302, https://doi.org/10.1029/97WR02766, 1998.

Virtanen, P., Gommers, R., Oliphant, T. E., Haberland, M., Reddy, T., Cournapeau, D., Burovski, E., Peterson, P., Weckesser, W., Bright, J., Van Der Walt, S. J., Brett, M., Wilson, J., Millman, K. J., Mayorov, N., Nelson, A. R. J., Jones, E., Kern, R., Larson, E., Carey, C. J., Polat, İ., Feng, Y., Moore, E. W., VanderPlas, J., Laxalde, D., Perktold, J., Cimrman, R., Henriksen, I., Quintero, E. A., Harris, C. R., Archibald, A. M., Ribeiro, A. H., Pedregosa, F., Van Mulbregt, P., SciPy 1.0 Contributors, Vijaykumar, A., Bardelli, A. P., Rothberg, A., Hilboll, A., Kloeckner, A., Scopatz, A., Lee, A., Rokem, A., Woods, C. N., Fulton, C., Masson, C., Häggström, C., Fitzgerald, C., Nicholson, D. A., Hagen, D. R., Pasechnik, D. V., Olivetti, E., Martin, E., Wieser, E., Silva, F., Lenders, F., Wilhelm, F., Young, G., Price, G. A., Ingold, G.-L., Allen, G. E., Lee, G. R., Audren, H., Probst, I., Dietrich, J. P., Silterra, J., Webber, J. T., Slavič, J., Nothman, J., Buchner, J., Kulick, J., Schönberger, J. L., De Miranda Cardoso, J. V., Reimer, J., Harrington, J., Rodríguez, J. L. C., Nunez-Iglesias, J., Kuczynski, J., Tritz, K., Thoma, M., Newville, M., Kümmerer, M., Bolingbroke, M., Tartre, M., Pak, M., Smith, N. J., Nowaczyk, N., Shebanov, N., Pavlyk, O., Brodtkorb, P. A., Lee, P., McGibbon, R. T., Feldbauer, R., Lewis, S., Tygier, S., Sievert, S., Vigna, S., Peterson, S., More, S., Pudlik, T., Oshima, T., Pingel, T. J., Robitaille, T. P., Spura, T., Jones, T. R., Cera, T., Leslie, T., Zito, T., Krauss, T., Upadhyay, U., Halchenko, Y. O., and Vázquez-Baeza, Y.: SciPy 1.0: fundamental algorithms for scientific computing in Python, Nature Methods, 17, 261–272, https://doi.org/10.1038/s41592-019-0686-2, 2020.

https://doi.org/10.5194/egusphere-2023-3118
Preprint. Discussion started: 8 January 2024

Wara, C., Thomas, M., Mwakurya, S., and Katuva, J.: Development of River Rating Curves for Simple to Complex Hydraulic Structure Based on Calibrated HEC-RAS Hydraulic Model, in Kwale, Coastal Kenya, Journal of Water Resource and Protection, 11, 468–490, https://doi.org/10.4236/jwarp.2019.114028, 2019.

Wickert, A. D.: doublemanning, https://doi.org/10.5281/zenodo.7495274, 2023.

Wickert, A. D. and Schildgen, T. F.: Long-profile evolution of transport-limited gravel-bed rivers, Earth Surface Dynamics, 7, 17–43, https://doi.org/10.5194/esurf-7-17-2019, 2019.

Wood, J.: Buried in bluff country: Stream and valley sedimentation in the Whitewater River Valley, Minnesota (USA), Master's thesis, University of Minnesota, Minneapolis, MN, USA, 2023.

World Meteorological Organization: Manual on stream gauging, Vol I: Fieldwork, no. 1044 in WMO, Secretariat of the World Meteorological Organization, Geneva, 2010a.

World Meteorological Organization: Manual on stream gauging, Vol II: Computation of discharge, no. 1044 in WMO, Secretariat of the World Meteorological Organization, Geneva, 2010b.

https://doi.org/10.5194/egusphere-2023-3118
Preprint. Discussion started: 8 January 2024

Table 2. Rivers used to test the double-Manning approach. All units are SI. Discharge start and end are for our calculation of mean discharge, and do not imply the loss of the stream gauge.

River	Minnesota	Cannon	La Dormida
Gauge			
Name	Jordan	Welch	Captación
Operator	USGS	USGS	–
Number	05330000	05355200	–
Latitude	44.69301845	44.5638559	−0.023482
Longitude	−93.641902	−92.7321429	−78.016396
Drainage area [m^2]	42000 $\times 10^6$	3470 $\times 10^6$	6.9 $\times 10^6$
Mean Discharge [$m^3\ s^{-1}$]	150	30	1.6
Discharge data start	1934.10.01	1991.10.01	2019.01.02
Discharge data end	2021.07.23	2019.08.19	2023.06.30
Rating-curve data points	1131	86	4
Rating-curve data start	1934.07.12	2002.01.08	2018.12.31
Rating-curve data end	2020.10.29	2012.01.19	2023.06.30
Measured			
Channel width (b) [m]	100	45	2.6
Valley-bottom width (B) [m]	1100	300	8.3
Channel depth (h) [m]	7	2.17 $\pm$0.33	0.7
Channel slope (S)	0.0001	0.0009	0.0788
Grain size (D_{50}) [m]	0.25 $\times 10^{-3}$	[a] 39 $\times 10^{-3}$	123 $\times 10^{-3}$
Grain size (D_{84}) [m]	0.35 $\times 10^{-3}$	[a] 55 $\times 10^{-3}$	180 $\times 10^{-3}$
Manning's n from D [$s\ m^{-1/3}$]	–	[a] ≤ 0.030	0.037
Solved			
Manning's n [$s\ m^{-1/3}$]	0.034	0.025	0.038
k_{fp} [$m^{3-P_{fp}}\ s^{-1}$]	138	39.7	[b] 11.4
P_{fp}	1.62	[c] 5/3	[d] 5/3
n_{fp} [$s\ m^{-1/3}$]	[b,e] 0.079	[b] 0.061	[f] 0.14
Stage Offset [m]	0.47	0.67	0.063
Channel depth [m]	5.8	2.1	[d] 0.7
Channel width [m]	[d] 100	[d] 45	[d] 2.6
Solution RMSE [$m^3\ s^{-1}$]	44.6	8.48	0.0245
RMSE / Mean Discharge	0.30	0.28	0.015

[a] Data obtained from bars at the confluence with a steep tributary ∼500 m upstream of the gauge. These likely represent a maximum grain size at the gauge itself, and therefore, likely upper limit on the in-channel Manning's n.
[b] Computed independently following Equation 10
[c] Fixed at boundary values during inversion
[d] Fixed by input data
[e] Back-calculated through a fit in which P_{fp} is fixed at 5/3.
[f] Fixed at estimated value from qualitative field observations